

RECEIVED: June 27, 2018

REVISED: August 24, 2018

ACCEPTED: September 27, 2018

PUBLISHED: October 12, 2018

Search for beautiful tetraquarks in the $\Upsilon(1S)\mu^+\mu^-$ invariant-mass spectrum



The LHCb collaboration

E-mail: dcraik@cern.ch

ABSTRACT: The $\Upsilon(1S)\mu^+\mu^-$ invariant-mass distribution is investigated for a possible exotic meson state composed of two b quarks and two \bar{b} quarks, $X_{b\bar{b}b\bar{b}}$. The analysis is based on a data sample of pp collisions recorded with the LHCb detector at centre-of-mass energies $\sqrt{s} = 7, 8$ and 13 TeV, corresponding to an integrated luminosity of 6.3 fb^{-1} . No significant excess is found, and upper limits are set on the product of the production cross-section and the branching fraction as functions of the mass of the $X_{b\bar{b}b\bar{b}}$ state. The limits are set in the fiducial volume where all muons have pseudorapidity in the range $[2.0, 5.0]$, and the $X_{b\bar{b}b\bar{b}}$ state has rapidity in the range $[2.0, 4.5]$ and transverse momentum less than $15 \text{ GeV}/c$.

KEYWORDS: B physics, Exotics, Hadron-Hadron scattering (experiments), Heavy quark production

ARXIV EPRINT: [1806.09707](https://arxiv.org/abs/1806.09707)

Contents

1	Introduction	1
2	Detector and simulation	2
3	Event selection	2
4	Invariant-mass fits	3
5	Normalisation factor	4
6	Systematic uncertainties	7
7	Limit setting	7
8	Conclusions	8
A	Additional material	9
	The LHCb collaboration	16

1 Introduction

Since the discovery of the $X(3872)$ state [1], over thirty exotic hadrons have been observed by several experiments (see refs. [2–7] for recent reviews). Most progress has been seen in the charmonium sector, where tetraquark (pentaquark) candidates with masses around $4\text{ GeV}/c^2$ have been found decaying to final states containing charmonia and are believed to have a minimal quark content of $c\bar{c}q\bar{q}'$ ($c\bar{c}qq'q''$), where q refers to a light quark (u, d, s). Two tetraquark states have also been seen in the bottomonium sector, via their decay to $\Upsilon\pi$ final states [8].

So far, no exotic hadron that is composed of more than two heavy quarks has been observed. However, there have recently been several predictions for the mass and width of an exotic state, $X_{b\bar{b}b\bar{b}}$ (denoted by X in the following), with quark composition $b\bar{b}b\bar{b}$ [9–19]. These predictions indicate that the X state would have a mass in the region $[18.4, 18.8]\text{ GeV}/c^2$, placing it close to, but typically below, the $\eta_b\eta_b$ threshold of $18.798 \pm 0.005\text{ GeV}/c^2$ [20], which implies that it could decay to $\Upsilon\ell^+\ell^-$ ($\ell = e, \mu$) final states. Further motivation is provided by the recent observation of $\Upsilon(1S)\Upsilon(1S)$ production by the CMS collaboration [21]. Possible search strategies for the X state have been outlined in ref. [22], and the product of its production cross-section at the LHC and the branching fraction to four muons is estimated to be of $\mathcal{O}(1\text{ fb})$. However, recent lattice QCD calculations do not find evidence for such a state in the hadron spectrum [23].

The current paper presents the first search for this state decaying to $\Upsilon(1S)\mu^+\mu^-$ through a study of the four-muon invariant-mass distribution, $m(2\mu^+2\mu^-)$, between 17.5 and $20.0\text{ GeV}/c^2$. The dataset consists of pp collision data recorded by the LHCb experiment at centre-of-mass energies of $\sqrt{s} = 7\text{ TeV}$, 8 TeV and 13 TeV between 2011 and 2017. The corresponding integrated luminosities are 1.0 fb^{-1} , 2.0 fb^{-1} and 3.3 fb^{-1} , respectively. The $\Upsilon(1S) \rightarrow \mu^+\mu^-$ decay is used as a normalisation channel to calculate the X production cross-section relative to that of the $\Upsilon(1S)$ meson.

2 Detector and simulation

The LHCb detector [24, 25] is a single-arm forward spectrometer covering the pseudorapidity range $2 < \eta < 5$, designed for the study of particles containing b or c quarks. The detector includes a high-precision tracking system consisting of a silicon-strip vertex detector surrounding the pp interaction region, a large-area silicon-strip detector located upstream of a dipole magnet with a bending power of about 4 Tm , and three stations of silicon-strip detectors and straw drift tubes placed downstream of the magnet. The tracking system provides a measurement of the momentum, p , of charged particles with a relative uncertainty that varies from 0.5% at low momentum to 1.0% at $200\text{ GeV}/c$. The minimum distance of a track to a primary vertex (PV), the impact parameter (IP), is measured with a resolution of $(15 + 29/p_T)\text{ }\mu\text{m}$, where p_T is the component of the momentum transverse to the beam, in GeV/c . Different types of charged hadrons are distinguished using information from two ring-imaging Cherenkov detectors. Photons, electrons and hadrons are identified by a calorimeter system consisting of scintillating-pad and preshower detectors, an electromagnetic calorimeter and a hadronic calorimeter. Muons are identified by a system composed of alternating layers of iron and multiwire proportional chambers [26].

Simulated datasets are used to evaluate reconstruction and selection efficiencies of the $\Upsilon(1S)$ and X decays studied in this paper. In the simulation, pp collisions are generated using PYTHIA [27, 28] with a specific LHCb configuration [29]. Decays of hadronic particles are described by EVTGEN [30], in which final-state radiation is generated using PHOTOS [31]. The interaction of the generated particles with the detector, and its response, are implemented using the GEANT4 toolkit [32, 33] as described in ref. [34]. The X state is produced using the same production model as the $\Upsilon(4S)$ meson, with the mass changed to one of three values in the range $18\,450 - 18\,830\text{ MeV}/c^2$. The natural width of the X state is assumed to be $1.2\text{ MeV}/c^2$ and its decay to the $\Upsilon(1S)\mu^+\mu^-$ final state is modelled by a phase-space distribution. The kinematic distribution of simulated X particles is shown in appendix A.

3 Event selection

For both signal and normalisation channels, the $\Upsilon(1S) \rightarrow \mu^+\mu^-$ candidates are first required to pass the trigger [35], which consists of a hardware stage, based on information from the calorimeter and muon systems, followed by a software stage, which applies a full event reconstruction. At the hardware level, a minimum requirement is placed on the product of

the transverse momenta of the two muons. At the software level, requirements are made on the total and transverse momentum of these muons, the dimuon invariant mass and on the quality of the dimuon vertex fit. Additionally, requirements are placed on the track quality of the muons and on particle identification (PID) quantities of the muons.

In the offline selection, all muons are required to have $p \in [8, 500] \text{ GeV}/c$, p_T larger than $1 \text{ GeV}/c$ and $\eta \in [2.0, 5.0]$. Stringent requirements are also applied to muon track-quality and PID quantities to reduce backgrounds from particles that are misidentified as muons. For both signal and normalisation channels, all muons are required to be consistent with originating from a common PV. The $\Upsilon(1S) \rightarrow \mu^+ \mu^-$ candidates are required to have invariant masses $m(\mu^+ \mu^-) \in [8.5, 11.5] \text{ GeV}/c^2$ and a good vertex-fit quality.

For the $X \rightarrow \Upsilon(1S) \mu^+ \mu^-$ decay, the $\Upsilon(1S)$ candidates are combined with an additional dimuon pair with a good vertex-fit quality. In addition to the four-muon vertex fit having good quality, the X candidates are required to have invariant masses $m(2\mu^+ 2\mu^-) \in [16.0, 22.0] \text{ GeV}/c^2$, rapidities in the range $[2.0, 4.5]$ and p_T less than $15 \text{ GeV}/c$. If a same-charge pair of muons has an invariant mass less than $220 \text{ MeV}/c^2$ or an opening angle smaller than 0.002 radians, then the corresponding X candidate is removed. This requirement eliminates pairs of muon candidates that are wrongly reconstructed from one single track. Candidates are also rejected if the combination of either muon from the $\Upsilon(1S)$ decay with the oppositely charged additional muon has an invariant mass consistent with that of the J/ψ meson, $m(\mu^+ \mu^-) \in [3050, 3150] \text{ MeV}/c^2$. The signal sample is a subset of the normalisation sample, smaller by a factor of $\mathcal{O}(10^4)$.

Multiple X candidates are seen in approximately 10% of events that pass the full selection and have $m(\mu^+ \mu^-)$ within $\pm 100 \text{ MeV}/c^2$ of the known $\Upsilon(1S)$ mass [20]. These are mostly due to the same $\Upsilon(1S)$ candidate being combined with different additional dimuons. These candidates are retained and treated as combinatorial background. Events with multiple candidates in the normalization $\Upsilon(1S)$ dataset occur at a negligible level.

4 Invariant-mass fits

Unbinned extended maximum-likelihood fits are made to the $m(2\mu^+ 2\mu^-)$ and $m(\mu^+ \mu^-)$ distributions to determine X and $\Upsilon(1S)$ yields, respectively. Fits to three datasets collected at pp centre-of-mass energies of $\sqrt{s} = 7 \text{ TeV}$ in 2011, 8 TeV in 2012 and 13 TeV in 2015–2017 are performed. In addition, a fit is made to a merged dataset that combines all 7, 8 and 13 TeV subsets. In each fit, the combinatorial background component is described by an exponential function with the slope and normalisation as free parameters. Signal components are described by Crystal Ball functions [36] with the tail parameters fixed to values obtained from fits to the simulated samples.

In fits to the $m(\mu^+ \mu^-)$ distributions, contributions from the $\Upsilon(1S)$, $\Upsilon(2S)$ and $\Upsilon(3S)$ states are included. For the $\Upsilon(1S)$ contribution, the mean, $\mu_{\Upsilon(1S)}$, and width, $\sigma_{\Upsilon(1S)}$, of the shape are free parameters. For the $\Upsilon(nS)$ contributions ($n = 2, 3$) the means are free parameters while each width is fixed to that of the $\Upsilon(1S)$ component scaled by the ratio of the $\Upsilon(1S)$ and $\Upsilon(nS)$ masses. The number of candidates of each component is free in each fit.

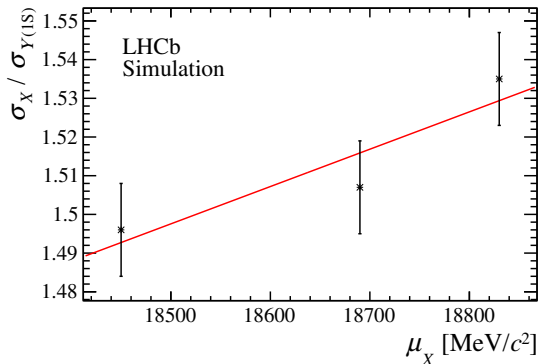


Figure 1. Linear fit to the ratio of the X and $\Upsilon(1S)$ widths as a function of the X mass as determined from fits to simulated data samples. The error bars represent the statistical uncertainty arising from the finite size of the simulated samples.

In the fits to the $m(2\mu^+2\mu^-)$ distributions, the mean of the X contribution, μ_X , takes a value in the range $[17.5, 20.0] \text{ GeV}/c^2$, while the width, σ_X , is calculated as the product of the corresponding $\Upsilon(1S)$ resolution and a linear X -mass-dependent scaling factor [37], $\sigma_X = k(\mu_X) \times \sigma_{\Upsilon(1S)}$ with $k(\mu_X) = p_0 + p_1(\mu_X - 18\,690 \text{ MeV}/c^2)$. The values of the $\Upsilon(1S)$ resolution and the two coefficients of the linear function are constrained by Gaussian functions. The constraints on the $\Upsilon(1S)$ resolution, taken from fits to the normalisation datasets, are 44.00 ± 0.05 , 44.307 ± 0.035 , 43.155 ± 0.023 and $43.766 \pm 0.018 \text{ MeV}/c^2$ for the 7, 8, 13 TeV and combined datasets, respectively. The constraints on p_0 and p_1 are 1.516 ± 0.007 and $(9.6 \pm 4.4) \times 10^{-5} (\text{MeV}/c^2)^{-1}$, respectively, evaluated from a fit to the simulated data, as shown in figure 1. These constraints lead to typical X resolutions in the range $\sim [60, 70] \text{ MeV}/c^2$.

The fits to the $m(\mu^+\mu^-)$ distributions in the normalisation datasets are shown in figure 2. The fitted $\Upsilon(1S)$ yields in the range $R_{\Upsilon(1S)} \equiv \mu_{\Upsilon(1S)} \pm 2.5\sigma_{\Upsilon(1S)}$ are $(0.694 \pm 0.012) \times 10^6$, $(1.562 \pm 0.028) \times 10^6$, $(4.11 \pm 0.08) \times 10^6$ and $(6.37 \pm 0.12) \times 10^6$ for the 7, 8, 13 TeV and combined datasets, respectively. The uncertainties include systematic components due to the choice of shapes to describe the signal and background components. Only candidates in the signal dataset with $m(\mu^+\mu^-)$ in the range $R_{\Upsilon(1S)}$ are retained for the fits to the distributions of $m(2\mu^+2\mu^-)$, which includes a small fraction of non- $\Upsilon(1S)$ background. Background-only fits to the signal datasets are shown in figure 3. No significant signal excess is observed. The largest deviation occurs at a mass of approximately $19.35 \text{ GeV}/c^2$, above the $\eta_b\eta_b$ and $\Upsilon(1S)\Upsilon(1S)$ thresholds, with a local significance of 2.5 standard deviations.

5 Normalisation factor

Upper limits are set for different X mass hypotheses on the quantity

$$S \equiv \sigma(pp \rightarrow X) \times \mathcal{B}(X \rightarrow \Upsilon(1S)\mu^+\mu^-) \times \mathcal{B}(\Upsilon(1S) \rightarrow \mu^+\mu^-), \quad (5.1)$$

where $\sigma(pp \rightarrow X)$ is the X production cross-section, and $\mathcal{B}(X \rightarrow \Upsilon(1S)\mu^+\mu^-)$ and $\mathcal{B}(\Upsilon(1S) \rightarrow \mu^+\mu^-)$ are the branching fractions of the $X \rightarrow \Upsilon(1S)\mu^+\mu^-$ and $\Upsilon(1S) \rightarrow \mu^+\mu^-$

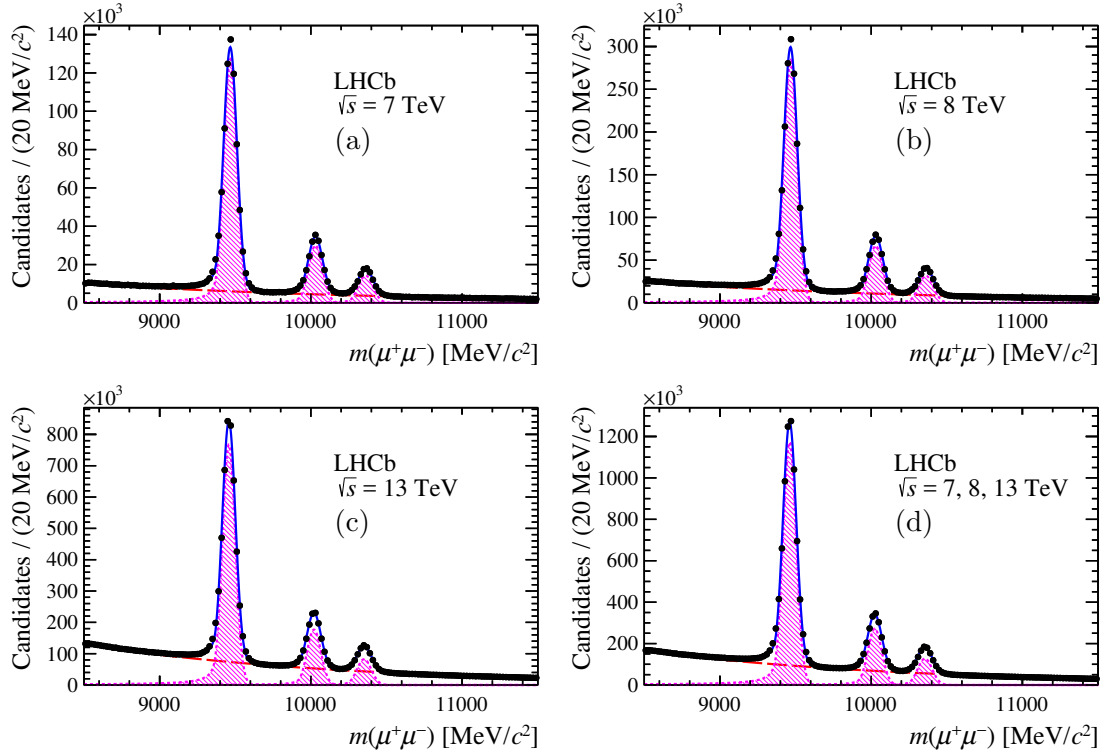


Figure 2. Distributions of $m(\mu^+\mu^-)$ for the normalisation datasets at pp centre-of-mass energies of (a) 7 TeV, (b) 8 TeV, (c) 13 TeV and (d) all combined. The total fit function (solid blue line), the combinatorial background (dashed red line) and the $\Upsilon(1S)$, $\Upsilon(2S)$ and $\Upsilon(3S)$ components (hatched magenta area) are shown overlaid.

decays, respectively. To set limits on S , the signal yield is parameterised as $N_{\text{sig}} = S/f_{\text{norm}}$ with

$$f_{\text{norm}} = \frac{\sigma(pp \rightarrow \Upsilon(1S)) \times \mathcal{B}(\Upsilon(1S) \rightarrow \mu^+\mu^-)}{N_{\text{norm}}} \times \frac{\epsilon_{\text{norm}}}{\epsilon_{\text{sig}}}, \quad (5.2)$$

where $\sigma(pp \rightarrow \Upsilon(1S))$ is the production cross-section of the $\Upsilon(1S)$ meson [38, 39] within the same fiducial volume as the signal. The $\Upsilon(1S) \rightarrow \mu^+\mu^-$ yield within the range $R_{\Upsilon(1S)}$ is given by N_{norm} , and $\epsilon_{\text{sig(norm)}}$ is the efficiency with which the signal (normalisation) channel is triggered, reconstructed and selected.

The relative efficiency of the reconstruction and selection requirements placed on the corresponding signal and normalisation datasets is defined as

$$\frac{\epsilon_{\text{sig}}}{\epsilon_{\text{norm}}} = \frac{\epsilon_{\text{sig}}^{\text{geom}}}{\epsilon_{\text{norm}}^{\text{geom}}} \times \frac{\epsilon_{\text{sig}}^{\text{sel}}}{\epsilon_{\text{norm}}^{\text{sel}}} \times \epsilon_{\text{sig}}^{\text{PID}} \times f_{\text{sig}}^{\text{trk}}, \quad (5.3)$$

where ϵ^{geom} is the efficiency with which the products of the X or $\Upsilon(1S)$ decay all enter the LHCb geometric acceptance; ϵ^{sel} is the efficiency of the reconstruction and selection of X or $\Upsilon(1S)$ candidates within the geometric acceptance; $\epsilon_{\text{sig}}^{\text{PID}}$ is the efficiency of the PID requirements placed on the additional muons in the signal decay; and $f_{\text{sig}}^{\text{trk}}$ accounts for

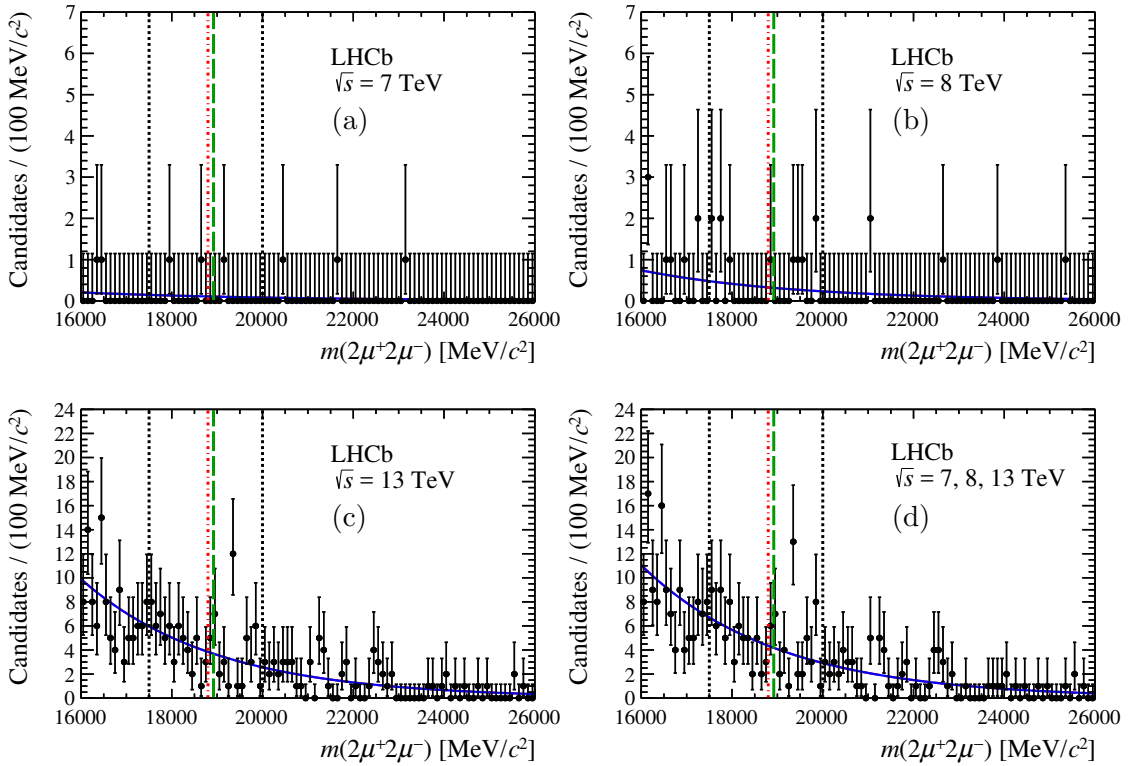


Figure 3. Distributions of $m(2\mu^+2\mu^-)$ for the signal datasets at pp centre-of-mass energies of (a) 7 TeV, (b) 8 TeV, (c) 13 TeV and (d) all combined, using a bin size comparable to the expected X mass resolution. In each case the region around the corresponding $\Upsilon(1S)$ peak has been selected. The background-only fit function (solid blue line) is shown overlaid. The dotted black lines indicate the range in which limits are set on the product of the X production cross-section and branching fractions. The dash-dotted red and long-dashed green lines show the positions of the $\eta_b\eta_b$ and $\Upsilon(1S)\Upsilon(1S)$ thresholds, respectively.

differences between data and simulation in the tracking efficiency of the additional muons. The geometric and selection efficiencies are determined from simulated samples, while the PID efficiency is determined from calibration data samples. The ratio of efficiencies between the signal and normalisation samples is determined to be $31.7 \pm 0.6\%$ ($35.2 \pm 1.2\%$) for the 7, 8 TeV (13 TeV) dataset, where the same efficiency is used for 7 and 8 TeV collisions due to the similar performance of the LHCb detector during these operational periods.

Uncertainties on these quantities give rise to systematic uncertainties in the fits to the signal datasets and enter these fits as a Gaussian function constraining the value of f_{norm} . These systematic uncertainties are detailed further in section 6. In the case of the combined dataset, averages of the efficiency ratio and normalisation cross-section, weighted by the integrated luminosity of each subset, are used to calculate f_{norm} . The values of f_{norm} are 11.1 ± 1.5 , 6.49 ± 0.25 , 3.27 ± 0.24 and 1.82 ± 0.10 fb for the 7, 8, 13 TeV and combined datasets, respectively.

6 Systematic uncertainties

Systematic uncertainties are included in the fits to the distribution of $m(2\mu^+2\mu^-)$ through additional Gaussian terms in the likelihood function that constrain the values of four nuisance parameters: f_{norm} , $\sigma_{\Upsilon(1S)}$, p_0 and p_1 . Uncertainties on the normalisation yields, the $\Upsilon(1S)$ production cross-sections, and the relative efficiencies of the signal and normalisation channels all contribute to the uncertainty on the f_{norm} parameter. The uncertainty on $\sigma_{\Upsilon(1S)}$ is obtained from the fit to the $m(\mu^+\mu^-)$ distribution of the normalisation channel. The linear coefficients of the X -mass-dependent resolution scale term are constrained according to the uncertainties on these parameters from fits to simulated data.

The relative uncertainties on the $\sigma_{\Upsilon(1S)}$, p_0 and p_1 parameters are $\lesssim 0.1\%$, 0.5% and 46% , respectively. Since these parameters are weakly correlated with the signal yield their effects on the measured cross-section upper limits are negligible. The uncertainty on the f_{norm} parameter for each dataset is dominated by uncertainties on the normalisation cross-section (2.8 to 6.3%) and the tracking efficiency correction (0.8 to 3.1%). The systematic uncertainties from efficiencies related to particle identification or geometrical acceptance are at the level of 1.0% or less. For the 7 TeV result, a discrepancy is observed in the efficiency- and cross-section-corrected $\Upsilon(1S)$ yield relative to the other datasets. An additional uncertainty of 13.5% is assigned to account for this. This uncertainty increases the limits on the cross section at 7 TeV by $< 4\%$ and has no effect on the quoted combined limits. The limits reported on the X production cross-section are all statistically dominated.

7 Limit setting

For each signal dataset, upper limits are set on S as functions of the X mass, μ_X , in the range [17.5, 20.0] GeV/ c^2 using the following procedure. For each fixed X mass, the likelihood profile as a function of S is integrated to determine upper limits on the cross-section at 90% and 95% confidence levels (CL). This procedure is applied at each of 101 values of the X mass. The 90% and 95% CL limits are tabulated in appendix A. Background-only pseudoexperiments are generated at each scan point to determine the expected 95% CL upper limit and corresponding one and two standard deviation intervals, as shown in figure 4. No significant excess is seen at any mass hypothesis for any dataset.

The analysis is repeated with only a single candidate decay retained for each event (chosen at random), with a more stringent requirement on the pseudorapidity of the muons as was previously used in ref. [40]. In addition, the effect of the assumption that the X decays according to a phase-space distribution is tested by evaluating the efficiency for both $m(\mu^+\mu^-)$ less than 2 GeV/ c^2 and $m(\mu^+\mu^-)$ greater than 7 GeV/ c^2 for the muon pairs that do not come from the $\Upsilon(1S)$ decay. The efficiency varies $\pm 24\%$ with respect to the total efficiency under the assumption of a phase-space decay. Finally, the limits are evaluated using different ranges around the $\Upsilon(1S)$ mass to select the signal dataset, separately for each year of the $\sqrt{s} = 13$ TeV dataset, and for the 7 and 8 TeV datasets combined. No significant differences are observed in the limits determined in each of these cross-checks.

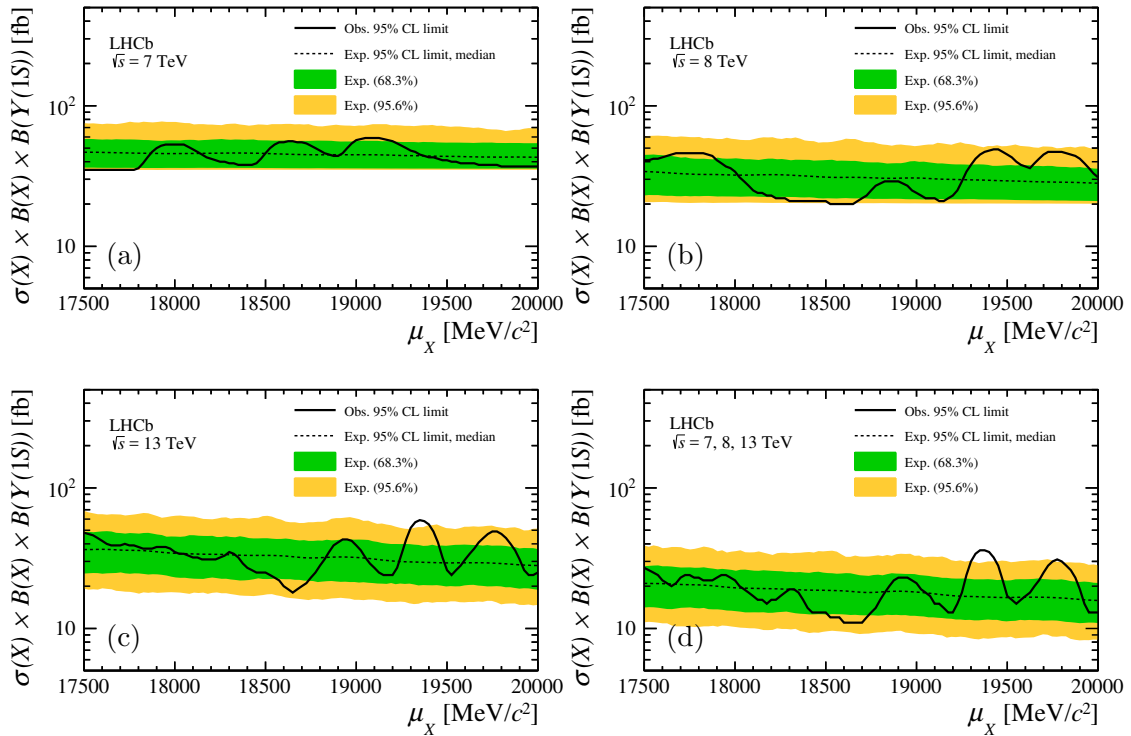


Figure 4. The 95 % CL upper limits on $S \equiv \sigma(pp \rightarrow X) \times \mathcal{B}(X \rightarrow \Upsilon(1S)\mu^+\mu^-) \times \mathcal{B}(\Upsilon(1S) \rightarrow \mu^+\mu^-)$ as functions of the X mass hypothesis at pp centre-of-mass energies of (a) 7 TeV, (b) 8 TeV and (c) 13 TeV and (d) all combined.

8 Conclusions

In conclusion, a search is performed for the decay of the beautiful tetraquark, X , to the $\Upsilon(1S)\mu^+\mu^-$ final state. No significant excess is seen for any mass hypothesis in the range $[17.5, 20.0]\text{ GeV}/c^2$. Upper limits are set on the value of $\sigma(pp \rightarrow X) \times \mathcal{B}(X \rightarrow \Upsilon(1S)\mu^+\mu^-) \times \mathcal{B}(\Upsilon(1S) \rightarrow \mu^+\mu^-)$ at centre-of-mass energies $\sqrt{s} = 7\text{ TeV}$, 8 TeV and 13 TeV as functions of the X mass hypothesis (see appendix). An upper limit is also set on the combined dataset using the average of the $\Upsilon(1S)$ cross-section, weighted by the integrated luminosity of each subset, resulting in upper limits of $\mathcal{O}(10\text{ fb})$. Improved sensitivity for this state will be obtained using data collected during future running periods of the LHC using an updated LHCb detector [41–43].

Acknowledgments

We express our gratitude to our colleagues in the CERN accelerator departments for the excellent performance of the LHC. We thank the technical and administrative staff at the LHCb institutes. We acknowledge support from CERN and from the national agencies: CAPES, CNPq, FAPERJ and FINEP (Brazil); MOST and NSFC (China); CNRS/IN2P3 (France); BMBF, DFG and MPG (Germany); INFN (Italy); NWO (Netherlands); MNiSW and NCN (Poland); MEN/IFA (Romania); MinES and FASO (Russia); MinECo (Spain);

SNSF and SER (Switzerland); NASU (Ukraine); STFC (United Kingdom); NSF (U.S.A.). We acknowledge the computing resources that are provided by CERN, IN2P3 (France), KIT and DESY (Germany), INFN (Italy), SURF (Netherlands), PIC (Spain), GridPP (United Kingdom), RRCKI and Yandex LLC (Russia), CSCS (Switzerland), IFIN-HH (Romania), CBPF (Brazil), PL-GRID (Poland) and OSC (U.S.A.). We are indebted to the communities behind the multiple open-source software packages on which we depend. Individual groups or members have received support from AvH Foundation (Germany), EPLANET, Marie Skłodowska-Curie Actions and ERC (European Union), ANR, Labex P2IO and OCEVU, and Région Auvergne-Rhône-Alpes (France), Key Research Program of Frontier Sciences of CAS, CAS PIFI, and the Thousand Talents Program (China), RFBR, RSF and Yandex LLC (Russia), GVA, XuntaGal and GENCAT (Spain), Herchel Smith Fund, the Royal Society, the English-Speaking Union and the Leverhulme Trust (United Kingdom).

A Additional material

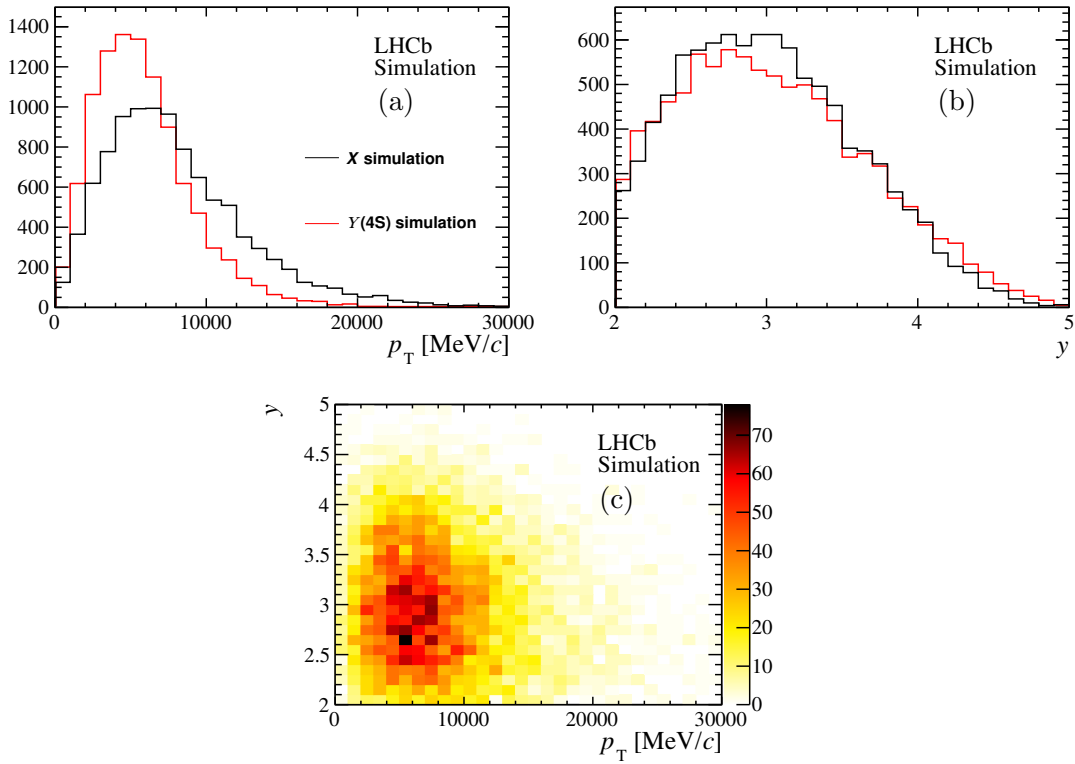


Figure 5. The kinematic distribution of (black) simulated X particles in (a) p_T and (b) rapidity, and (c) the 2D distribution. For comparison, the kinematic distribution of (red) simulated $\Upsilon(4S)$ particles is also shown.

Mass [MeV/ c^2]	Upper limit 90 % (95 %)			CL [fb]
	7 TeV	8 TeV	13 TeV	
17500	27 (35)	34 (41)	41 (48)	23 (27)
17525	27 (35)	34 (41)	40 (47)	23 (27)
17550	27 (35)	35 (42)	39 (46)	22 (26)
17575	27 (35)	35 (42)	37 (44)	20 (24)
17600	27 (35)	36 (43)	35 (42)	19 (23)
17625	27 (35)	36 (44)	33 (40)	17 (21)
17650	27 (35)	37 (45)	32 (39)	17 (21)
17675	27 (35)	38 (46)	32 (39)	18 (22)
17700	27 (35)	38 (46)	33 (39)	19 (23)
17725	27 (35)	38 (46)	33 (40)	20 (24)
17750	27 (35)	38 (46)	33 (39)	20 (24)
17775	27 (35)	38 (46)	32 (39)	20 (24)
17800	28 (36)	39 (46)	32 (38)	19 (23)
17825	29 (39)	38 (46)	31 (37)	19 (22)
17850	33 (43)	38 (45)	30 (37)	18 (22)
17875	37 (47)	36 (44)	30 (37)	18 (22)
17900	40 (50)	34 (41)	31 (38)	19 (23)
17925	42 (52)	32 (39)	32 (38)	20 (24)
17950	43 (53)	30 (37)	31 (38)	20 (24)
17975	43 (53)	29 (36)	30 (37)	19 (23)
18000	43 (53)	27 (34)	29 (35)	18 (22)
18025	43 (53)	25 (31)	28 (34)	17 (21)
18050	42 (53)	22 (29)	27 (34)	16 (19)
18075	41 (51)	21 (27)	27 (33)	15 (18)
18100	39 (49)	20 (25)	26 (32)	14 (17)
18125	37 (47)	19 (24)	26 (32)	13 (16)
18150	35 (45)	18 (24)	25 (31)	13 (16)
18175	34 (43)	18 (23)	25 (31)	13 (16)
18200	33 (42)	17 (23)	25 (31)	13 (16)
18225	32 (41)	17 (22)	25 (31)	13 (17)
18250	31 (40)	17 (22)	26 (32)	14 (18)
18275	30 (40)	17 (22)	28 (33)	15 (19)
18300	30 (39)	16 (21)	29 (35)	16 (19)
18325	30 (39)	16 (21)	28 (34)	16 (19)
18350	29 (38)	16 (21)	27 (32)	15 (18)
18375	29 (38)	16 (21)	24 (29)	13 (16)

Table 1. Upper limits on $\sigma(pp \rightarrow X) \times \mathcal{B}(X \rightarrow \Upsilon(1S)\mu^+\mu^-) \times \mathcal{B}(\Upsilon(1S) \rightarrow \mu^+\mu^-)$ for different X mass hypotheses in the range $[17.5, 18.4] \text{ GeV}/c^2$.

Mass [MeV/ c^2]	Upper limit 90 % (95 %)			CL (fb)
	7 TeV	8 TeV	13 TeV	
18400	29 (38)	16 (21)	22 (27)	11 (14)
18425	29 (38)	16 (21)	20 (26)	11 (13)
18450	30 (39)	16 (21)	20 (25)	10 (13)
18475	32 (42)	16 (21)	20 (25)	10 (13)
18500	36 (46)	16 (21)	20 (25)	10 (13)
18525	40 (50)	16 (20)	19 (24)	10 (13)
18550	43 (53)	16 (20)	18 (23)	10 (12)
18575	44 (55)	15 (20)	17 (22)	9 (12)
18600	45 (55)	15 (20)	16 (20)	9 (12)
18625	45 (56)	15 (20)	15 (19)	9 (11)
18650	45 (56)	16 (20)	14 (18)	8 (11)
18675	45 (55)	16 (21)	14 (19)	8 (11)
18700	44 (55)	17 (22)	15 (20)	9 (11)
18725	43 (54)	18 (23)	17 (21)	9 (12)
18750	42 (52)	20 (25)	18 (23)	10 (13)
18775	40 (50)	21 (27)	20 (25)	11 (14)
18800	38 (48)	22 (28)	23 (28)	13 (16)
18825	36 (46)	23 (29)	26 (31)	15 (18)
18850	35 (45)	23 (29)	29 (35)	17 (20)
18875	34 (44)	23 (29)	32 (39)	18 (22)
18900	34 (44)	23 (29)	35 (41)	20 (23)
18925	35 (46)	22 (28)	36 (43)	20 (24)
18950	39 (50)	21 (27)	37 (43)	20 (23)
18975	43 (54)	19 (25)	35 (42)	19 (22)
19000	46 (57)	18 (24)	33 (39)	18 (21)
19025	47 (58)	18 (23)	30 (36)	16 (20)
19050	48 (59)	17 (22)	26 (32)	15 (18)
19075	48 (59)	17 (22)	24 (29)	14 (17)
19100	48 (59)	16 (22)	22 (27)	13 (16)
19125	48 (59)	16 (21)	20 (25)	12 (15)
19150	48 (58)	16 (21)	19 (24)	11 (14)
19175	47 (57)	16 (22)	19 (24)	11 (14)
19200	46 (56)	17 (23)	19 (24)	11 (14)
19225	44 (54)	19 (25)	22 (27)	12 (15)
19250	41 (52)	23 (29)	27 (34)	15 (19)
19275	39 (50)	27 (34)	36 (43)	21 (25)

Table 2. Upper limits on $\sigma(pp \rightarrow X) \times \mathcal{B}(X \rightarrow \Upsilon(1S)\mu^+\mu^-) \times \mathcal{B}(\Upsilon(1S) \rightarrow \mu^+\mu^-)$ for different X mass hypotheses in the range [18.4, 19.3] GeV/ c^2 .

Mass [MeV/ c^2]	Upper limit 90 % (95 %)			CL (fb)
	7 TeV	8 TeV	13 TeV	
19300	38 (48)	31 (38)	45 (52)	27 (31)
19325	36 (47)	34 (42)	50 (57)	31 (35)
19350	35 (45)	37 (45)	52 (59)	32 (36)
19375	34 (44)	40 (47)	51 (58)	32 (36)
19400	33 (43)	41 (48)	48 (55)	31 (35)
19425	33 (43)	42 (49)	42 (49)	29 (32)
19450	32 (42)	41 (49)	34 (41)	24 (28)
19475	32 (41)	40 (47)	26 (32)	19 (22)
19500	31 (41)	38 (45)	21 (26)	14 (18)
19525	31 (40)	36 (43)	19 (24)	13 (16)
19550	31 (40)	33 (40)	20 (26)	13 (16)
19575	30 (39)	31 (38)	22 (28)	13 (16)
19600	30 (39)	29 (37)	25 (31)	14 (17)
19625	30 (39)	29 (36)	28 (34)	15 (19)
19650	29 (39)	31 (39)	31 (37)	17 (21)
19675	29 (38)	34 (42)	34 (41)	19 (23)
19700	29 (38)	37 (45)	38 (44)	22 (26)
19725	29 (38)	39 (47)	41 (47)	25 (29)
19750	29 (38)	40 (47)	42 (49)	27 (30)
19775	29 (38)	40 (47)	42 (49)	27 (31)
19800	29 (37)	39 (47)	41 (47)	26 (30)
19825	28 (37)	39 (46)	38 (44)	25 (28)
19850	28 (37)	38 (45)	34 (40)	22 (26)
19875	28 (37)	37 (44)	30 (36)	19 (23)
19900	28 (37)	35 (42)	25 (31)	16 (19)
19925	28 (37)	32 (39)	21 (26)	12 (16)
19950	28 (37)	29 (36)	19 (24)	11 (13)
19975	28 (37)	26 (33)	19 (24)	10 (13)
20000	28 (37)	24 (31)	20 (25)	11 (13)

Table 3. Upper limits on $\sigma(pp \rightarrow X) \times \mathcal{B}(X \rightarrow \Upsilon(1S)\mu^+\mu^-) \times \mathcal{B}(\Upsilon(1S) \rightarrow \mu^+\mu^-)$ for different X mass hypotheses in the range [19.3, 20.0] GeV/ c^2 .

Open Access. This article is distributed under the terms of the Creative Commons Attribution License ([CC-BY 4.0](#)), which permits any use, distribution and reproduction in any medium, provided the original author(s) and source are credited.

References

- [1] BELLE collaboration, S.K. Choi et al., *Observation of a narrow charmonium-like state in exclusive $B^\pm \rightarrow K^\pm \pi^+ \pi^- J/\psi$ decays*, *Phys. Rev. Lett.* **91** (2003) 262001 [[hep-ex/0309032](#)] [[INSPIRE](#)].
- [2] H.-X. Chen, W. Chen, X. Liu and S.-L. Zhu, *The hidden-charm pentaquark and tetraquark states*, *Phys. Rept.* **639** (2016) 1 [[arXiv:1601.02092](#)] [[INSPIRE](#)].
- [3] R.F. Lebed, R.E. Mitchell and E.S. Swanson, *Heavy-quark QCD exotica*, *Prog. Part. Nucl. Phys.* **93** (2017) 143 [[arXiv:1610.04528](#)] [[INSPIRE](#)].
- [4] A. Esposito, A. Pilloni and A.D. Polosa, *Multiquark resonances*, *Phys. Rept.* **668** (2016) 1 [[arXiv:1611.07920](#)] [[INSPIRE](#)].
- [5] F.-K. Guo et al., *Hadronic molecules*, *Rev. Mod. Phys.* **90** (2018) 015004 [[arXiv:1705.00141](#)] [[INSPIRE](#)].
- [6] A. Ali, J.S. Lange and S. Stone, *Exotics: heavy pentaquarks and tetraquarks*, *Prog. Part. Nucl. Phys.* **97** (2017) 123 [[arXiv:1706.00610](#)] [[INSPIRE](#)].
- [7] S.L. Olsen, T. Skwarnicki and D. Zieminska, *Nonstandard heavy mesons and baryons: experimental evidence*, *Rev. Mod. Phys.* **90** (2018) 015003 [[arXiv:1708.04012](#)] [[INSPIRE](#)].
- [8] BELLE collaboration, A. Bondar et al., *Observation of two charged bottomonium-like resonances in $\Upsilon(5S)$ decays*, *Phys. Rev. Lett.* **108** (2012) 122001 [[arXiv:1110.2251](#)] [[INSPIRE](#)].
- [9] L. Heller and J.A. Tjon, *On bound states of heavy $Q^2\bar{Q}^2$ systems*, *Phys. Rev. D* **32** (1985) 755 [[INSPIRE](#)].
- [10] A.V. Berezhnoy, A.V. Luchinsky and A.A. Novoselov, *Heavy tetraquarks production at the LHC*, *Phys. Rev. D* **86** (2012) 034004 [[arXiv:1111.1867](#)] [[INSPIRE](#)].
- [11] J. Wu et al., *Heavy-flavored tetraquark states with the $QQ\bar{Q}\bar{Q}$ configuration*, *Phys. Rev. D* **97** (2018) 094015 [[arXiv:1605.01134](#)] [[INSPIRE](#)].
- [12] W. Chen et al., *Hunting for exotic doubly hidden-charm/bottom tetraquark states*, *Phys. Lett. B* **773** (2017) 247 [[arXiv:1605.01647](#)] [[INSPIRE](#)].
- [13] M. Karliner, S. Nussinov and J.L. Rosner, *$QQ\bar{Q}\bar{Q}$ states: masses, production and decays*, *Phys. Rev. D* **95** (2017) 034011 [[arXiv:1611.00348](#)] [[INSPIRE](#)].
- [14] Y. Bai, S. Lu and J. Osborne, *Beauty-full tetraquarks*, [arXiv:1612.00012](#) [[INSPIRE](#)].
- [15] Z.-G. Wang, *Analysis of the $QQ\bar{Q}\bar{Q}$ tetraquark states with QCD sum rules*, *Eur. Phys. J. C* **77** (2017) 432 [[arXiv:1701.04285](#)] [[INSPIRE](#)].
- [16] J.-M. Richard, A. Valcarce and J. Vijande, *String dynamics and metastability of all-heavy tetraquarks*, *Phys. Rev. D* **95** (2017) 054019 [[arXiv:1703.00783](#)] [[INSPIRE](#)].
- [17] M.N. Anwar et al., *Spectroscopy and decays of the fully-heavy tetraquarks*, *Eur. Phys. J. C* **78** (2018) 647 [[arXiv:1710.02540](#)] [[INSPIRE](#)].

- [18] R. Vega-Morales and R. Vega-Morales, *Golden probe of the di- Υ threshold*, [arXiv:1710.02738](#) [INSPIRE].
- [19] W. Chen et al., *Doubly hidden-charm/bottom $QQ\bar{Q}\bar{Q}$ tetraquark states*, talk given at the 6th International Conference on New Frontiers in Physics (ICNFP 2017), August 17-26, Kolymbari, Crete, Greece (2017), [arXiv:1803.02522](#) [INSPIRE].
- [20] PARTICLE DATA GROUP collaboration, C. Patrignani et al., *Review of particle physics*, *Chin. Phys. C* **40** (2016) 100001 [[INSPIRE](#)].
- [21] CMS collaboration, *Observation of $\Upsilon(1S)$ pair production in proton-proton collisions at $\sqrt{s} = 8$ TeV*, *JHEP* **05** (2017) 013 [[arXiv:1610.07095](#)] [[INSPIRE](#)].
- [22] E. Eichten and Z. Liu, *Would a deeply bound $b\bar{b}b\bar{b}$ tetraquark meson be observed at the LHC?*, [arXiv:1709.09605](#) [INSPIRE].
- [23] C. Hughes, E. Eichten and C.T.H. Davies, *Searching for beauty-fully bound tetraquarks using lattice nonrelativistic QCD*, *Phys. Rev. D* **97** (2018) 054505 [[arXiv:1710.03236](#)] [[INSPIRE](#)].
- [24] LHCb collaboration, *The LHCb detector at the LHC*, 2008 *JINST* **3** S08005 [[INSPIRE](#)].
- [25] LHCb collaboration, *LHCb detector performance*, *Int. J. Mod. Phys. A* **30** (2015) 1530022 [[arXiv:1412.6352](#)] [[INSPIRE](#)].
- [26] A.A. Alves Jr. et al., *Performance of the LHCb muon system*, 2013 *JINST* **8** P02022 [[arXiv:1211.1346](#)] [[INSPIRE](#)].
- [27] T. Sjöstrand, S. Mrenna and P.Z. Skands, *A brief introduction to PYTHIA 8.1*, *Comput. Phys. Commun.* **178** (2008) 852 [[arXiv:0710.3820](#)] [[INSPIRE](#)].
- [28] T. Sjöstrand, S. Mrenna and P.Z. Skands, *PYTHIA 6.4 physics and manual*, *JHEP* **05** (2006) 026 [[hep-ph/0603175](#)] [[INSPIRE](#)].
- [29] I. Belyaev et al., *Handling of the generation of primary events in Gauss, the LHCb simulation framework*, *J. Phys. Conf. Ser.* **331** (2011) 032047 [[INSPIRE](#)].
- [30] D.J. Lange, *The EvtGen particle decay simulation package*, *Nucl. Instrum. Meth. A* **462** (2001) 152 [[INSPIRE](#)].
- [31] P. Golonka and Z. Was, *PHOTOS Monte Carlo: a precision tool for QED corrections in Z and W decays*, *Eur. Phys. J. C* **45** (2006) 97 [[hep-ph/0506026](#)] [[INSPIRE](#)].
- [32] GEANT4 collaboration, J. Allison et al., *GEANT4 developments and applications*, *IEEE Trans. Nucl. Sci.* **53** (2006) 270.
- [33] GEANT4 collaboration, S. Agostinelli et al., *GEANT4: a Simulation toolkit*, *Nucl. Instrum. Meth. A* **506** (2003) 250 [[INSPIRE](#)].
- [34] M. Clemencic et al., *The LHCb simulation application, gauss: design, evolution and experience*, *J. Phys. Conf. Ser.* **331** (2011) 032023 [[INSPIRE](#)].
- [35] R. Aaij et al., *The LHCb trigger and its performance in 2011*, 2013 *JINST* **8** P04022 [[arXiv:1211.3055](#)] [[INSPIRE](#)].
- [36] T. Skwarnicki, *A study of the radiative cascade transitions between the Υ' and Υ resonances*, Ph.D. thesis, Institute of Nuclear Physics, Krakow, Poland (1986), DESY-F31-86-02.
- [37] LHCb collaboration, *Measurement of the $B_s^0 \rightarrow \mu^+ \mu^-$ branching fraction and effective lifetime and search for $B^0 \rightarrow \mu^+ \mu^-$ decays*, *Phys. Rev. Lett.* **118** (2017) 191801 [[arXiv:1703.05747](#)] [[INSPIRE](#)].

- [38] LHCb collaboration, *Forward production of Υ mesons in pp collisions at $\sqrt{s} = 7$ and 8 TeV*, *JHEP* **11** (2015) 103 [[arXiv:1509.02372](#)] [[INSPIRE](#)].
- [39] LHCb collaboration, *Measurement of Υ production in pp collisions at $\sqrt{s} = 13$ TeV*, *JHEP* **07** (2018) 134 [[arXiv:1804.09214](#)] [[INSPIRE](#)].
- [40] LHCb collaboration, *Measurement of the Υ polarizations in pp collisions at $\sqrt{s} = 7$ and 8 TeV*, *JHEP* **12** (2017) 110 [[arXiv:1709.01301](#)] [[INSPIRE](#)].
- [41] LHCb collaboration, *Framework TDR for the LHCb upgrade: technical design report*, [CERN-LHCC-2012-007](#) (2012).
- [42] LHCb collaboration, *Expression of interest for a Phase-II LHCb upgrade: opportunities in flavour physics and beyond, in the HL-LHC era*, [CERN-LHCC-2017-003](#) (2017).
- [43] LHCb collaboration, *Physics case for an LHCb Upgrade II — Opportunities in flavour physics, and beyond, in the HL-LHC era*, [arXiv:1808.08865](#) [[LHCb-PUB-2018-009](#)].

The LHCb collaboration

R. Aaij²⁷, B. Adeva⁴¹, M. Adinolfi⁴⁸, C.A. Aidala⁷³, Z. Ajaltouni⁵, S. Akar⁵⁰, P. Albicocco¹⁸, J. Albrecht¹⁰, F. Alessio⁴², M. Alexander⁵³, A. Alfonso Albero⁴⁰, S. Ali²⁷, G. Alkhazov³³, P. Alvarez Cartelle⁵⁵, A.A. Alves Jr⁴¹, S. Amato², S. Amerio²³, Y. Amhis⁷, L. An³, L. Anderlini¹⁷, G. Andreassi⁴³, M. Andreotti^{16,g}, J.E. Andrews⁶⁰, R.B. Appleby⁵⁶, F. Archilli²⁷, P. d'Argent¹², J. Arnau Romeu⁶, A. Artamonov³⁹, M. Artuso⁶¹, K. Arzymatov³⁷, E. Aslanides⁶, M. Atzeni⁴⁴, B. Audurier²², S. Bachmann¹², J.J. Back⁵⁰, S. Baker⁵⁵, V. Balagura^{7,b}, W. Baldini¹⁶, A. Baranov³⁷, R.J. Barlow⁵⁶, S. Barsuk⁷, W. Barter⁵⁶, F. Baryshnikov⁷⁰, V. Batozskaya³¹, B. Batsukh⁶¹, V. Battista⁴³, A. Bay⁴³, J. Beddow⁵³, F. Bedeschi²⁴, I. Bediaga¹, A. Beiter⁶¹, L.J. Bel²⁷, S. Belin²², N. Beliy⁶³, V. Bellee⁴³, N. Belloli^{20,i}, K. Belous³⁹, I. Belyaev^{34,42}, E. Ben-Haim⁸, G. Bencivenni¹⁸, S. Benson²⁷, S. Beranek⁹, A. Berezhnoy³⁵, R. Bernet⁴⁴, D. Berninghoff¹², E. Bertholet⁸, A. Bertolin²³, C. Betancourt⁴⁴, F. Betti^{15,42}, M.O. Bettler⁴⁹, M. van Beuzekom²⁷, Ia. Bezshyiko⁴⁴, S. Bhasin⁴⁸, J. Bhom²⁹, S. Bifani⁴⁷, P. Billoir⁸, A. Birnkraut¹⁰, A. Bizzeti^{17,u}, M. Bjørn⁵⁷, M.P. Blago⁴², T. Blake⁵⁰, F. Blanc⁴³, S. Blusk⁶¹, D. Bobulska⁵³, V. Bocci²⁶, O. Boente Garcia⁴¹, T. Boettcher⁵⁸, A. Bondar^{38,w}, N. Bondar³³, S. Borghi^{56,42}, M. Borisjak³⁷, M. Borsato⁴¹, F. Bossu⁷, M. Boubdir⁹, T.J.V. Bowcock⁵⁴, C. Bozzi^{16,42}, S. Braun¹², M. Brodski⁴², J. Brodzicka²⁹, A. Brossa Gonzalo⁵⁰, D. Brundu²², E. Buchanan⁴⁸, A. Buonaura⁴⁴, C. Burr⁵⁶, A. Bursche²², J. Buytaert⁴², W. Byczynski⁴², S. Cadeddu²², H. Cai⁶⁴, R. Calabrese^{16,g}, R. Calladine⁴⁷, M. Calvi^{20,i}, M. Calvo Gomez^{40,m}, A. Camboni^{40,m}, P. Campana¹⁸, D.H. Campora Perez⁴², L. Capriotti⁵⁶, A. Carbone^{15,e}, G. Carboni²⁵, R. Cardinale^{19,h}, A. Cardini²², P. Carniti^{20,i}, L. Carson⁵², K. Carvalho Akiba², G. Casse⁵⁴, L. Cassina²⁰, M. Cattaneo⁴², G. Cavallero^{19,h}, R. Cenci^{24,p}, D. Chamont⁷, M.G. Chapman⁴⁸, M. Charles⁸, Ph. Charpentier⁴², G. Chatzikonstantinidis⁴⁷, M. Chefdeville⁴, V. Chekalina³⁷, C. Chen³, S. Chen²², S.-G. Chitic⁴², V. Chobanova⁴¹, M. Chrzaszcz⁴², A. Chubykin³³, P. Ciambrone¹⁸, X. Cid Vidal⁴¹, G. Ciezarek⁴², P.E.L. Clarke⁵², M. Clemencic⁴², H.V. Cliff⁴⁹, J. Closier⁴², V. Coco⁴², J.A.B. Coelho⁷, J. Cogan⁶, E. Cogneras⁵, L. Cojocariu³², P. Collins⁴², T. Colombo⁴², A. Comerma-Montells¹², A. Contu²², G. Coombs⁴², S. Coquereau⁴⁰, G. Corti⁴², M. Corvo^{16,g}, C.M. Costa Sobral⁵⁰, B. Couturier⁴², G.A. Cowan⁵², D.C. Craik⁵⁸, A. Crocombe⁵⁰, M. Cruz Torres¹, R. Currie⁵², C. D'Ambrosio⁴², F. Da Cunha Marinho², C.L. Da Silva⁷⁴, E. Dall'Occo²⁷, J. Dalseno⁴⁸, A. Danilina³⁴, A. Davis³, O. De Aguiar Francisco⁴², K. De Bruyn⁴², S. De Capua⁵⁶, M. De Cian⁴³, J.M. De Miranda¹, L. De Paula², M. De Serio^{14,d}, P. De Simone¹⁸, C.T. Dean⁵³, D. Decamp⁴, L. Del Buono⁸, B. Delaney⁴⁹, H.-P. Dembinski¹¹, M. Demmer¹⁰, A. Dendek³⁰, D. Derkach³⁷, O. Deschamps⁵, F. Desse⁷, F. Dettori⁵⁴, B. Dey⁶⁵, A. Di Canto⁴², P. Di Nezza¹⁸, S. Didenko⁷⁰, H. Dijkstra⁴², F. Dordei⁴², M. Dorigo^{42,y}, A. Dosil Suárez⁴¹, L. Douglas⁵³, A. Dovbnya⁴⁵, K. Dreimanis⁵⁴, L. Dufour²⁷, G. Dujany⁸, P. Durante⁴², J.M. Durham⁷⁴, D. Dutta⁵⁶, R. Dzhelyadin³⁹, M. Dziewiecki¹², A. Dziurda²⁹, A. Dzyuba³³, S. Easo⁵¹, U. Egede⁵⁵, V. Egorychev³⁴, S. Eidelman^{38,w}, S. Eisenhardt⁵², U. Eitschberger¹⁰, R. Ekelhof¹⁰, L. Eklund⁵³, S. Ely⁶¹, A. Ene³², S. Escher⁹, S. Esen²⁷, T. Evans⁵⁹, A. Falabella¹⁵, N. Farley⁴⁷, S. Farry⁵⁴, D. Fazzini^{20,42,i}, L. Federici²⁵, P. Fernandez Declara⁴², A. Fernandez Prieto⁴¹, F. Ferrari¹⁵, L. Ferreira Lopes⁴³, F. Ferreira Rodrigues², M. Ferro-Luzzi⁴², S. Filippov³⁶, R.A. Fini¹⁴, M. Fiorini^{16,g}, M. Firlej³⁰, C. Fitzpatrick⁴³, T. Fiutowski³⁰, F. Fleuret^{7,b}, M. Fontana^{22,42}, F. Fontanelli^{19,h}, R. Forty⁴², V. Franco Lima⁵⁴, M. Frank⁴², C. Frei⁴², J. Fu^{21,q}, W. Funk⁴², C. Färber⁴², M. Féo Pereira Rivello Carvalho²⁷, E. Gabriel⁵², A. Gallas Torreira⁴¹, D. Galli^{15,e}, S. Gallorini²³, S. Gambetta⁵², Y. Gan³, M. Gandelman², P. Gandini²¹, Y. Gao³, L.M. Garcia Martin⁷², B. Garcia Plana⁴¹, J. García Pardiñas⁴⁴, J. Garra Tico⁴⁹, L. Garrido⁴⁰, D. Gascon⁴⁰, C. Gaspar⁴², L. Gavardi¹⁰, G. Gazzoni⁵, D. Gerick¹², E. Gersabeck⁵⁶,

- M. Gersabeck⁵⁶, T. Gershon⁵⁰, D. Gerstel⁶, Ph. Ghez⁴, S. Giani⁴³, V. Gibson⁴⁹, O.G. Girard⁴³, L. Giubega³², K. Gizdov⁵², V.V. Gligorov⁸, D. Golubkov³⁴, A. Golutvin^{55,70}, A. Gomes^{1,a}, I.V. Gorelov³⁵, C. Gotti^{20,i}, E. Govorkova²⁷, J.P. Grabowski¹², R. Graciani Diaz⁴⁰, L.A. Granado Cardoso⁴², E. Graugés⁴⁰, E. Graverini⁴⁴, G. Graziani¹⁷, A. Grecu³², R. Greim²⁷, P. Griffith²², L. Grillo⁵⁶, L. Gruber⁴², B.R. Gruberg Cazon⁵⁷, O. Grünberg⁶⁷, C. Gu³, E. Gushchin³⁶, Yu. Guz^{39,42}, T. Gys⁴², C. Göbel⁶², T. Hadavizadeh⁵⁷, C. Hadjivasilou⁵, G. Haefeli⁴³, C. Haen⁴², S.C. Haines⁴⁹, B. Hamilton⁶⁰, X. Han¹², T.H. Hancock⁵⁷, S. Hansmann-Menzemer¹², N. Harnew⁵⁷, S.T. Harnew⁴⁸, T. Harrison⁵⁴, C. Hasse⁴², M. Hatch⁴², J. He⁶³, M. Hecker⁵⁵, K. Heinicke¹⁰, A. Heister¹⁰, K. Hennessy⁵⁴, L. Henry⁷², E. van Herwijnen⁴², M. Heß⁶⁷, A. Hicheur², R. Hidalgo Charman⁵⁶, D. Hill⁵⁷, M. Hilton⁵⁶, P.H. Hopchev⁴³, W. Hu⁶⁵, W. Huang⁶³, Z.C. Huard⁵⁹, W. Hulsbergen²⁷, T. Humair⁵⁵, M. Hushchyn³⁷, D. Hutchcroft⁵⁴, D. Hynds²⁷, P. Ibis¹⁰, M. Idzik³⁰, P. Ilten⁴⁷, K. Ivshin³³, R. Jacobsson⁴², J. Jalocha⁵⁷, E. Jans²⁷, A. Jawahery⁶⁰, F. Jiang³, M. John⁵⁷, D. Johnson⁴², C.R. Jones⁴⁹, C. Joram⁴², B. Jost⁴², N. Jurik⁵⁷, S. Kandybei⁴⁵, M. Karacson⁴², J.M. Kariuki⁴⁸, S. Karodia⁵³, N. Kazeev³⁷, M. Kecke¹², F. Keizer⁴⁹, M. Kelsey⁶¹, M. Kenzie⁴⁹, T. Ketel²⁸, E. Khairullin³⁷, B. Khanji¹², C. Khurewathanakul⁴³, K.E. Kim⁶¹, T. Kirn⁹, S. Klaver¹⁸, K. Klimaszewski³¹, T. Klimkovich¹¹, S. Koliev⁴⁶, M. Kolpin¹², R. Kopecna¹², P. Koppenburg²⁷, I. Kostiuk²⁷, S. Kotriakhova³³, M. Kozeiha⁵, L. Kravchuk³⁶, M. Kreps⁵⁰, F. Kress⁵⁵, P. Krokovny^{38,w}, W. Krupa³⁰, W. Krzemien³¹, W. Kucewicz^{29,l}, M. Kucharczyk²⁹, V. Kudryavtsev^{38,w}, A.K. Kuonen⁴³, T. Kvaratskheliya^{34,42}, D. Lacarrere⁴², G. Lafferty⁵⁶, A. Lai²², D. Lancierini⁴⁴, G. Lanfranchi¹⁸, C. Langenbruch⁹, T. Latham⁵⁰, C. Lazzeroni⁴⁷, R. Le Gac⁶, A. Leflat³⁵, J. Lefrançois⁷, R. Lefèvre⁵, F. Lemaitre⁴², O. Leroy⁶, T. Lesiak²⁹, B. Leverington¹², P.-R. Li⁶³, T. Li³, Z. Li⁶¹, X. Liang⁶¹, T. Likhomanenko⁶⁹, R. Lindner⁴², F. Lionetto⁴⁴, V. Lisovskyi⁷, X. Liu³, D. Loh⁵⁰, A. Loi²², I. Longstaff⁵³, J.H. Lopes², G.H. Lovell⁴⁹, D. Lucchesi^{23,o}, M. Lucio Martinez⁴¹, A. Lupato²³, E. Luppi^{16,g}, O. Lupton⁴², A. Lusiani²⁴, X. Lyu⁶³, F. Machefert⁷, F. Maciuc³², V. Macko⁴³, P. Mackowiak¹⁰, S. Maddrell-Mander⁴⁸, O. Maev^{33,42}, K. Maguire⁵⁶, D. Maisuzenko³³, M.W. Majewski³⁰, S. Malde⁵⁷, B. Malecki²⁹, A. Malinin⁶⁹, T. Maltsev^{38,w}, G. Manca^{22,f}, G. Mancinelli⁶, D. Marangotto^{21,q}, J. Maratas^{5,v}, J.F. Marchand⁴, U. Marconi¹⁵, C. Marin Benito⁷, M. Marinangeli⁴³, P. Marino⁴³, J. Marks¹², P.J. Marshall⁵⁴, G. Martellotti²⁶, M. Martin⁶, M. Martinelli⁴², D. Martinez Santos⁴¹, F. Martinez Vidal⁷², A. Massafferri¹, M. Materok⁹, R. Matev⁴², A. Mathad⁵⁰, Z. Mathe⁴², C. Matteuzzi²⁰, A. Mauri⁴⁴, E. Maurice^{7,b}, B. Maurin⁴³, A. Mazurov⁴⁷, M. McCann^{55,42}, A. McNab⁵⁶, R. McNulty¹³, J.V. Mead⁵⁴, B. Meadows⁵⁹, C. Meaux⁶, F. Meier¹⁰, N. Meinert⁶⁷, D. Melnychuk³¹, M. Merk²⁷, A. Merli^{21,q}, E. Michielin²³, D.A. Milanes⁶⁶, E. Millard⁵⁰, M.-N. Minard⁴, L. Minzoni^{16,g}, D.S. Mitzel¹², A. Mogini⁸, J. Molina Rodriguez^{1,z}, T. Mombächer¹⁰, I.A. Monroy⁶⁶, S. Monteil⁵, M. Morandin²³, G. Morello¹⁸, M.J. Morello^{24,t}, O. Morgunova⁶⁹, J. Moron³⁰, A.B. Morris⁶, R. Mountain⁶¹, F. Muheim⁵², M. Mulder²⁷, C.H. Murphy⁵⁷, D. Murray⁵⁶, A. Mödden¹⁰, D. Müller⁴², J. Müller¹⁰, K. Müller⁴⁴, V. Müller¹⁰, P. Naik⁴⁸, T. Nakada⁴³, R. Nandakumar⁵¹, A. Nandi⁵⁷, T. Nanut⁴³, I. Nasteva², M. Needham⁵², N. Neri²¹, S. Neubert¹², N. Neufeld⁴², M. Neuner¹², T.D. Nguyen⁴³, C. Nguyen-Mau^{43,n}, S. Nieswand⁹, R. Niet¹⁰, N. Nikitin³⁵, A. Nogay⁶⁹, N.S. Nolte⁴², D.P. O'Hanlon¹⁵, A. Oblakowska-Mucha³⁰, V. Obraztsov³⁹, S. Ogilvy¹⁸, R. Oldeman^{22,f}, C.J.G. Onderwater⁶⁸, A. Ossowska²⁹, J.M. Otalora Goicochea², P. Owen⁴⁴, A. Oyanguren⁷², P.R. Pais⁴³, T. Pajero^{24,t}, A. Palano¹⁴, M. Palutan^{18,42}, G. Pashnин⁷¹, A. Papanestis⁵¹, M. Pappagallo⁵², L.L. Pappalardo^{16,g}, W. Parker⁶⁰, C. Parkes⁵⁶, G. Passaleva^{17,42}, A. Pastore¹⁴, M. Patel⁵⁵, C. Patrignani^{15,e}, A. Pearce⁴², A. Pellegrino²⁷, G. Penso²⁶, M. Pepe Altarelli⁴², S. Perazzini⁴², D. Pereima³⁴, P. Perret⁵, L. Pescatore⁴³, K. Petridis⁴⁸, A. Petrolini^{19,h}, A. Petrov⁶⁹, S. Petrucci⁵², M. Petruzzo^{21,q}, B. Pietrzyk⁴, G. Pietrzyk⁴³, M. Pikies²⁹, M. Pili⁵⁷, D. Pinci²⁶, J. Pinzino⁴², F. Pisani⁴², A. Piucci¹², V. Placinta³², S. Playfer⁵², J. Plews⁴⁷,

- M. Plo Casasus⁴¹, F. Polci⁸, M. Poli Lener¹⁸, A. Poluektov⁵⁰, N. Polukhina^{70,c}, I. Polyakov⁶¹, E. Polycarpo², G.J. Pomery⁴⁸, S. Ponce⁴², A. Popov³⁹, D. Popov^{47,11}, S. Poslavskii³⁹, C. Potterat², E. Price⁴⁸, J. Prisciandaro⁴¹, C. Prouve⁴⁸, V. Pugatch⁴⁶, A. Puig Navarro⁴⁴, H. Pullen⁵⁷, G. Punzi^{24,p}, W. Qian⁶³, J. Qin⁶³, R. Quagliani⁸, B. Quintana⁵, B. Rachwal³⁰, J.H. Rademacker⁴⁸, M. Rama²⁴, M. Ramos Pernas⁴¹, M.S. Rangel², F. Ratnikov^{37,x}, G. Raven²⁸, M. Ravonel Salzgeber⁴², M. Reboud⁴, F. Redi⁴³, S. Reichert¹⁰, A.C. dos Reis¹, F. Reiss⁸, C. Remon Alepuz⁷², Z. Ren³, V. Renaudin⁷, S. Ricciardi⁵¹, S. Richards⁴⁸, K. Rinnert⁵⁴, P. Robbe⁷, A. Robert⁸, A.B. Rodrigues⁴³, E. Rodrigues⁵⁹, J.A. Rodriguez Lopez⁶⁶, M. Roehrken⁴², A. Rogozhnikov³⁷, S. Roiser⁴², A. Rollings⁵⁷, V. Romanovskiy³⁹, A. Romero Vidal⁴¹, M. Rotondo¹⁸, M.S. Rudolph⁶¹, T. Ruf⁴², J. Ruiz Vidal⁷², J.J. Saborido Silva⁴¹, N. Sagidova³³, B. Saitta^{22,f}, V. Salustino Guimaraes⁶², C. Sanchez Gras²⁷, C. Sanchez Mayordomo⁷², B. Sanmartin Sedes⁴¹, R. Santacesaria²⁶, C. Santamarina Rios⁴¹, M. Santimaria¹⁸, E. Santovetti^{25,j}, G. Sarpis⁵⁶, A. Sarti^{18,k}, C. Satriano^{26,s}, A. Satta²⁵, M. Saur⁶³, D. Savrina^{34,35}, S. Schael⁹, M. Schellenberg¹⁰, M. Schiller⁵³, H. Schindler⁴², M. Schmelling¹¹, T. Schmelzer¹⁰, B. Schmidt⁴², O. Schneider⁴³, A. Schopper⁴², H.F. Schreiner⁵⁹, M. Schubiger⁴³, M.H. Schune⁷, R. Schwemmer⁴², B. Sciascia¹⁸, A. Sciubba^{26,k}, A. Semennikov³⁴, E.S. Sepulveda⁸, A. Sergi^{47,42}, N. Serra⁴⁴, J. Serrano⁶, L. Sestini²³, A. Seuthe¹⁰, P. Seyfert⁴², M. Shapkin³⁹, Y. Shcheglov^{33,†}, T. Shears⁵⁴, L. Shekhtman^{38,w}, V. Shevchenko⁶⁹, E. Shmanin⁷⁰, B.G. Siddi¹⁶, R. Silva Coutinho⁴⁴, L. Silva de Oliveira², G. Simi^{23,o}, S. Simone^{14,d}, N. Skidmore¹², T. Skwarnicki⁶¹, J.G. Smeaton⁴⁹, E. Smith⁹, I.T. Smith⁵², M. Smith⁵⁵, M. Soares¹⁵, I. Soares Lavra¹, M.D. Sokoloff⁵⁹, F.J.P. Soler⁵³, B. Souza De Paula², B. Spaan¹⁰, P. Spradlin⁵³, F. Stagni⁴², M. Stahl¹², S. Stahl⁴², P. Steffko⁴³, S. Stefkova⁵⁵, O. Steinkamp⁴⁴, S. Stemmle¹², O. Stenyakin³⁹, M. Stepanova³³, H. Stevens¹⁰, A. Stocchi⁷, S. Stone⁶¹, B. Storaci⁴⁴, S. Stracka^{24,p}, M.E. Stramaglia⁴³, M. Straticiuc³², U. Straumann⁴⁴, S. Strokov⁷¹, J. Sun³, L. Sun⁶⁴, K. Swientek³⁰, V. Syropoulos²⁸, T. Szumlak³⁰, M. Szymanski⁶³, S. T'Jampens⁴, Z. Tang³, A. Tayduganov⁶, T. Tekampe¹⁰, G. Tellarini¹⁶, F. Teubert⁴², E. Thomas⁴², J. van Tilburg²⁷, M.J. Tilley⁵⁵, V. Tisserand⁵, M. Tobin³⁰, S. Tolk⁴², L. Tomassetti^{16,g}, D. Tonelli²⁴, D.Y. Tou⁸, R. Tourinho Jadallah Aoude¹, E. Tournefier⁴, M. Traill⁵³, M.T. Tran⁴³, A. Trisovic⁴⁹, A. Tsaregorodtsev⁶, G. Tuci²⁴, A. Tully⁴⁹, N. Tuning^{27,42}, A. Ukleja³¹, A. Usachov⁷, A. Ustyuzhanin³⁷, U. Uwer¹², A. Vagner⁷¹, V. Vagnoni¹⁵, A. Valassi⁴², S. Valat⁴², G. Valenti¹⁵, R. Vazquez Gomez⁴², P. Vazquez Regueiro⁴¹, S. Vecchi¹⁶, M. van Veghel²⁷, J.J. Velthuis⁴⁸, M. Veltri^{17,r}, G. Veneziano⁵⁷, A. Venkateswaran⁶¹, T.A. Verlage⁹, M. Vernet⁵, M. Veronesi²⁷, N.V. Veronika¹³, M. Vesterinen⁵⁷, J.V. Viana Barbosa⁴², D. Vieira⁶³, M. Vieites Diaz⁴¹, H. Viemann⁶⁷, X. Vilasis-Cardona^{40,m}, A. Vitkovskiy²⁷, M. Vitti⁴⁹, V. Volkov³⁵, A. Vollhardt⁴⁴, B. Voneki⁴², A. Vorobyev³³, V. Vorobьев^{38,w}, J.A. de Vries²⁷, C. Vázquez Sierra²⁷, R. Waldi⁶⁷, J. Walsh²⁴, J. Wang⁶¹, M. Wang³, Y. Wang⁶⁵, Z. Wang⁴⁴, D.R. Ward⁴⁹, H.M. Wark⁵⁴, N.K. Watson⁴⁷, D. Websdale⁵⁵, A. Weiden⁴⁴, C. Weisser⁵⁸, M. Whitehead⁹, J. Wicht⁵⁰, G. Wilkinson⁵⁷, M. Wilkinson⁶¹, I. Williams⁴⁹, M.R.J. Williams⁵⁶, M. Williams⁵⁸, T. Williams⁴⁷, F.F. Wilson^{51,42}, J. Wimberley⁶⁰, M. Winn⁷, J. Wishahi¹⁰, W. Wislicki³¹, M. Witek²⁹, G. Wormser⁷, S.A. Wotton⁴⁹, K. Wyllie⁴², D. Xiao⁶⁵, Y. Xie⁶⁵, A. Xu³, M. Xu⁶⁵, Q. Xu⁶³, Z. Xu³, Z. Xu⁴, Z. Yang³, Z. Yang⁶⁰, Y. Yao⁶¹, L.E. Yeomans⁵⁴, H. Yin⁶⁵, J. Yu^{65,ab}, X. Yuan⁶¹, O. Yushchenko³⁹, K.A. Zarebski⁴⁷, M. Zavertyaev^{11,c}, D. Zhang⁶⁵, L. Zhang³, W.C. Zhang^{3,aa}, Y. Zhang⁷, A. Zhelezov¹², Y. Zheng⁶³, X. Zhu³, V. Zhukov^{9,35}, J.B. Zonneveld⁵², S. Zucchelli¹⁵

¹ Centro Brasileiro de Pesquisas Físicas (CBPF), Rio de Janeiro, Brazil² Universidade Federal do Rio de Janeiro (UFRJ), Rio de Janeiro, Brazil³ Center for High Energy Physics, Tsinghua University, Beijing, China⁴ Univ. Grenoble Alpes, Univ. Savoie Mont Blanc, CNRS, IN2P3-LAPP, Annecy, France

- ⁵ Clermont Université, Université Blaise Pascal, CNRS/IN2P3, LPC, Clermont-Ferrand, France
- ⁶ Aix Marseille Univ, CNRS/IN2P3, CPPM, Marseille, France
- ⁷ LAL, Univ. Paris-Sud, CNRS/IN2P3, Université Paris-Saclay, Orsay, France
- ⁸ LPNHE, Sorbonne Université, Paris Diderot Sorbonne Paris Cité, CNRS/IN2P3, Paris, France
- ⁹ I. Physikalisches Institut, RWTH Aachen University, Aachen, Germany
- ¹⁰ Fakultät Physik, Technische Universität Dortmund, Dortmund, Germany
- ¹¹ Max-Planck-Institut für Kernphysik (MPIK), Heidelberg, Germany
- ¹² Physikalisches Institut, Ruprecht-Karls-Universität Heidelberg, Heidelberg, Germany
- ¹³ School of Physics, University College Dublin, Dublin, Ireland
- ¹⁴ INFN Sezione di Bari, Bari, Italy
- ¹⁵ INFN Sezione di Bologna, Bologna, Italy
- ¹⁶ INFN Sezione di Ferrara, Ferrara, Italy
- ¹⁷ INFN Sezione di Firenze, Firenze, Italy
- ¹⁸ INFN Laboratori Nazionali di Frascati, Frascati, Italy
- ¹⁹ INFN Sezione di Genova, Genova, Italy
- ²⁰ INFN Sezione di Milano-Bicocca, Milano, Italy
- ²¹ INFN Sezione di Milano, Milano, Italy
- ²² INFN Sezione di Cagliari, Monserrato, Italy
- ²³ INFN Sezione di Padova, Padova, Italy
- ²⁴ INFN Sezione di Pisa, Pisa, Italy
- ²⁵ INFN Sezione di Roma Tor Vergata, Roma, Italy
- ²⁶ INFN Sezione di Roma La Sapienza, Roma, Italy
- ²⁷ Nikhef National Institute for Subatomic Physics, Amsterdam, Netherlands
- ²⁸ Nikhef National Institute for Subatomic Physics and VU University Amsterdam, Amsterdam, Netherlands
- ²⁹ Henryk Niewodniczanski Institute of Nuclear Physics Polish Academy of Sciences, Kraków, Poland
- ³⁰ AGH - University of Science and Technology, Faculty of Physics and Applied Computer Science, Kraków, Poland
- ³¹ National Center for Nuclear Research (NCBJ), Warsaw, Poland
- ³² Horia Hulubei National Institute of Physics and Nuclear Engineering, Bucharest-Magurele, Romania
- ³³ Petersburg Nuclear Physics Institute (PNPI), Gatchina, Russia
- ³⁴ Institute of Theoretical and Experimental Physics (ITEP), Moscow, Russia
- ³⁵ Institute of Nuclear Physics, Moscow State University (SINP MSU), Moscow, Russia
- ³⁶ Institute for Nuclear Research of the Russian Academy of Sciences (INR RAS), Moscow, Russia
- ³⁷ Yandex School of Data Analysis, Moscow, Russia
- ³⁸ Budker Institute of Nuclear Physics (SB RAS), Novosibirsk, Russia
- ³⁹ Institute for High Energy Physics (IHEP), Protvino, Russia
- ⁴⁰ ICCUB, Universitat de Barcelona, Barcelona, Spain
- ⁴¹ Instituto Galego de Física de Altas Enerxías (IGFAE), Universidade de Santiago de Compostela, Santiago de Compostela, Spain
- ⁴² European Organization for Nuclear Research (CERN), Geneva, Switzerland
- ⁴³ Institute of Physics, Ecole Polytechnique Fédérale de Lausanne (EPFL), Lausanne, Switzerland
- ⁴⁴ Physik-Institut, Universität Zürich, Zürich, Switzerland
- ⁴⁵ NSC Kharkiv Institute of Physics and Technology (NSC KIPT), Kharkiv, Ukraine
- ⁴⁶ Institute for Nuclear Research of the National Academy of Sciences (KINR), Kyiv, Ukraine
- ⁴⁷ University of Birmingham, Birmingham, United Kingdom
- ⁴⁸ H.H. Wills Physics Laboratory, University of Bristol, Bristol, United Kingdom
- ⁴⁹ Cavendish Laboratory, University of Cambridge, Cambridge, United Kingdom
- ⁵⁰ Department of Physics, University of Warwick, Coventry, United Kingdom
- ⁵¹ STFC Rutherford Appleton Laboratory, Didcot, United Kingdom
- ⁵² School of Physics and Astronomy, University of Edinburgh, Edinburgh, United Kingdom

- ⁵³ School of Physics and Astronomy, University of Glasgow, Glasgow, United Kingdom
⁵⁴ Oliver Lodge Laboratory, University of Liverpool, Liverpool, United Kingdom
⁵⁵ Imperial College London, London, United Kingdom
⁵⁶ School of Physics and Astronomy, University of Manchester, Manchester, United Kingdom
⁵⁷ Department of Physics, University of Oxford, Oxford, United Kingdom
⁵⁸ Massachusetts Institute of Technology, Cambridge, MA, United States
⁵⁹ University of Cincinnati, Cincinnati, OH, United States
⁶⁰ University of Maryland, College Park, MD, United States
⁶¹ Syracuse University, Syracuse, NY, United States
⁶² Pontifícia Universidade Católica do Rio de Janeiro (PUC-Rio), Rio de Janeiro, Brazil,
 associated to²
⁶³ University of Chinese Academy of Sciences, Beijing, China, associated to³
⁶⁴ School of Physics and Technology, Wuhan University, Wuhan, China, associated to³
⁶⁵ Institute of Particle Physics, Central China Normal University, Wuhan, Hubei, China,
 associated to³
⁶⁶ Departamento de Fisica , Universidad Nacional de Colombia, Bogota, Colombia, associated to⁸
⁶⁷ Institut für Physik, Universität Rostock, Rostock, Germany, associated to¹²
⁶⁸ Van Swinderen Institute, University of Groningen, Groningen, Netherlands, associated to²⁷
⁶⁹ National Research Centre Kurchatov Institute, Moscow, Russia, associated to³⁴
⁷⁰ National University of Science and Technology “MISIS”, Moscow, Russia, associated to³⁴
⁷¹ National Research Tomsk Polytechnic University, Tomsk, Russia, associated to³⁴
⁷² Instituto de Fisica Corpuscular, Centro Mixto Universidad de Valencia — CSIC, Valencia, Spain,
 associated to⁴⁰
⁷³ University of Michigan, Ann Arbor, United States, associated to⁶¹
⁷⁴ Los Alamos National Laboratory (LANL), Los Alamos, United States, associated to⁶¹
- ^a Universidade Federal do Triângulo Mineiro (UFTM), Uberaba-MG, Brazil
^b Laboratoire Leprince-Ringuet, Palaiseau, France
^c P.N. Lebedev Physical Institute, Russian Academy of Science (LPI RAS), Moscow, Russia
^d Università di Bari, Bari, Italy
^e Università di Bologna, Bologna, Italy
^f Università di Cagliari, Cagliari, Italy
^g Università di Ferrara, Ferrara, Italy
^h Università di Genova, Genova, Italy
ⁱ Università di Milano Bicocca, Milano, Italy
^j Università di Roma Tor Vergata, Roma, Italy
^k Università di Roma La Sapienza, Roma, Italy
^l AGH — University of Science and Technology, Faculty of Computer Science, Electronics and
 Telecommunications, Kraków, Poland
^m LIFAELS, La Salle, Universitat Ramon Llull, Barcelona, Spain
ⁿ Hanoi University of Science, Hanoi, Vietnam
^o Università di Padova, Padova, Italy
^p Università di Pisa, Pisa, Italy
^q Università degli Studi di Milano, Milano, Italy
^r Università di Urbino, Urbino, Italy
^s Università della Basilicata, Potenza, Italy
^t Scuola Normale Superiore, Pisa, Italy
^u Università di Modena e Reggio Emilia, Modena, Italy
^v MSU — Iligan Institute of Technology (MSU-IIT), Iligan, Philippines
^w Novosibirsk State University, Novosibirsk, Russia
^x National Research University Higher School of Economics, Moscow, Russia
^y Sezione INFN di Trieste, Trieste, Italy

^{*z*} Escuela Agrícola Panamericana, San Antonio de Oriente, Honduras

^{*aa*} School of Physics and Information Technology, Shaanxi Normal University (SNNU), Xi'an, China

^{*ab*} Physics and Micro Electronic College, Hunan University, Changsha City, China

† Deceased